Developmental Biology 351 (2011) 229–241

Contents lists available at ScienceDirect

Developmental Biology

journal homepage: www.elsevier.com/developmentalbiology

Disruption of planar cell polarity activity leads to developmental biliary defects

Shuang Cui [a], Louis M. Capecci [a], Randolph P. Matthews [a,b,*]

[a] Division of Gastroenterology, Hepatology, and Nutrition, The Children's Hospital of Philadelphia, Philadelphia, PA, USA
[b] Department of Pediatrics, University of Pennsylvania School of Medicine, Philadelphia, PA 19104, USA

ARTICLE INFO

Article history:
Received for publication 9 November 2009
Revised 15 December 2010
Accepted 22 December 2010
Available online 4 January 2011

ABSTRACT

Planar cell polarity (PCP) establishes polarity within an epithelial sheet. Defects in PCP are associated with developmental defects involving directional cell growth, including defects in kidney tubule elongation that lead to formation of kidney cysts. Given the strong association between kidney cyst formation and developmental biliary defects in patients and in animal models, we investigated the importance of PCP in biliary development. Here we report that in zebrafish, morpholino antisense oligonucleotide-mediated knockdown of PCP genes including *prickle-1a* (*pk1a*) led to developmental biliary abnormalities, as well as localization defects of the liver and other digestive organs. The defects in biliary development appear to be mediated via downstream PCP targets such as Rho kinase, Jun kinase (JNK), and both actin and microtubule components of the cytoskeleton. Knockdown of *pk1a* led to decreased expression of *vhnf1*, a homeodomain gene previously shown to be involved in biliary development and in kidney cyst formation; forced expression of *vhnf1* mRNA led to rescue of the *pk1a* morphant phenotype. Our results demonstrate that PCP plays an important role in vertebrate biliary development, interacting with other factors known to be involved in biliary morphogenesis.

Introduction

Planar cell polarity (PCP) is an essential property of multicellular tissues, mediating polarity within the epithelial plane perpendicular to apical–basal polarity. PCP involves noncanonical Wnt signaling, in which transmembrane receptors Frizzled, Strabismus (Vangl in vertebrates), or Flamingo (Celsr) recruit the adaptor protein Dishevelled (Dsh), which in turn activates the Jun kinase-Rac-Rho pathway to alter cytoskeletal dynamics and gene expression. Other conserved PCP components include the soluble factors Prickle (Pk) and Diego (Ankrd6 in vertebrates). The Flamingo/Strabismus/Prickle complex is generally located on the proximal side of an epithelial cell, while the Flamingo/Frizzled/Dishevelled/Diego complex is on the distal side, although Prickle acts on this complex as well (Zallen, 2007).

Defects in PCP signaling lead to several migration-related developmental defects, including defects in gastrulation (Takeuchi et al., 2003; Wallingford et al., 2000), islet cell migration into the pancreas, neuroepithelial migration into the eye, and the development of stereocilia in the inner ear (Karner et al., 2006). Defective signaling via PCP family members leads to the generation of renal cysts due to a role in directional tubule elongation during kidney development (Fischer et al., 2006; Saburi et al., 2008). We were intrigued by this observation, as there is a strong association between kidney cysts and abnormalities in intrahepatic biliary development. Ductal plate malformations, which are thought to represent abnormalities in intrahepatic biliary development (Desmet, 1998), are seen in autosomal recessive polycystic kidney disease, as well as in other genetic conditions such as Bardet–Biedl syndrome, Jeune asphyxiating thoracic dysplasia, and Meckel–Gruber syndrome, which also demonstrate cystic kidneys (Maclean and Dunwoodie, 2004).

Zebrafish have been well established as a model to study hepatobiliary development. While intrahepatic biliary development in zebrafish does not proceed via a ductal plate intermediate stage, there is otherwise strong conservation in terms of overall developmental process and in specific genetic pathways important in both zebrafish and mammalian biliary development. Apical–basal polarity of the hepatocyte is established prior to formation of the initial intrahepatic ducts (Sakaguchi et al., 2008), which lengthen and then remodel to become an interconnected lattice that drains the liver by 5 dpf (days post fertilization) (Lorent et al., 2010; Lorent et al., 2004; Matthews et al., 2004). Mediators of intrahepatic bile duct formation in mammals, such as *Onecut* family members (Clotman et al., 2005; Clotman et al., 2002), the homeodomain transcription factor *Hnf1b* (*vhnf1* in zebrafish) (Coffinier et al., 2002), and *Jagged* and *Notch* (Kodama et al., 2004; Lozier et al., 2008), also function in zebrafish biliary development (Lorent et al., 2010; Lorent et al., 2004; Matthews et al., 2008; Matthews et al., 2004). Thus, we tested our hypothesis that inhibition of PCP negatively affects biliary development using zebrafish.

* Corresponding author. Department of Pediatrics, University of Pennsylvania School of Medicine, Philadelphia, PA 19104, USA. Fax: +1 267 426 7814.
E-mail address: matthews@email.chop.edu (R.P. Matthews).

0012-1606/$ – see front matter © 2011 Elsevier Inc. All rights reserved.
doi:10.1016/j.ydbio.2010.12.041

In this study, we examined the expression pattern of PCP genes in zebrafish, and verified their expression in the developing liver during biliary growth and remodeling. Knockdown of *pk1a* and other PCP genes using morpholino antisense oligonucleotides demonstrated impaired bile duct formation, and also led to defects in left-right localization of digestive organs. Inhibitors of downstream targets of PCP such as Rho kinase and JNK also elicited biliary defects, supporting a role for PCP in biliary development. Furthermore, *vhnf1* expression was decreased in *pk1a* morphants, and forced expression of *vhnf1* rescued the biliary defects seen in *pk1a* morphants. These studies demonstrate for the first time that PCP genes are essential for biliary development.

Materials and methods

Animal care

Zebrafish were raised and housed in accordance with standard procedures, under protocols approved by the Institutional Animal Care and Use Committees (IACUCs) of The Children's Hospital of Philadelphia and the University of Pennsylvania. All wild-type fish used for these studies were top long fin (TLF).

In situ hybridization

Antisense riboprobes for *pk1a, dsh2, vangl2, dsh3, wnt11, wnt11r, ankrd6, prickle2, celsr1, celsr2, celsr3*, ceruloplasmin (*cp*), *fabp2*, trypsin (*try*) and insulin (*ins*) were synthesized directly from PCR products by using a T3 sequence that had been synthesized at the 5' end of the reverse primer (see Supplementary Table 1 for primer sequences). The PCR product was purified and then used as template for riboprobe synthesis as per standard protocols. The remainder of the in situ protocol was essentially as described previously (Wallace and Pack, 2003), using larvae raised in phenylthiourea (PTU) to inhibit the development of pigment, as per standard protocols.

Morpholino oligonucleotides and drug treatments

Morpholino oligonucleotides (MOs) were designed based on sequences available from the zebrafish genome assembly. All MOs were obtained from GeneTools (http://www.gene-tools.com; Philomath, OR), including standard and random control MOs. Morpholinos were designed to target the 5' translational start site and the splice acceptor site for exon 7 of the *pk1a* gene, for the 5' end and splice donor site of exon 1 for *vangl2*, and for the 5' translational start site and splice acceptor site for exon 2 for *ankrd6* (Table S1). The *hnf6* MOs have been detailed previously (Matthews et al., 2004). For all morpholinos, 1.5 ng was injected at the one-cell stage or at 48 hpf. Injections at 48 hpf were into the yolk, similar to previous studies (Matthews et al., 2009; Stenkamp and Frey, 2003). Injection with either the ATG or splice blocking MOs produced identical phenotypes, and knockdown was confirmed using 1.5 ng MO, by PCR or by western blot using antibodies directed against Prickle (Santa Cruz) (Fig. S1). For the epistasis experiments with *pk1a* MO and colchicine or cytochalasin D, 0.38 ng MO was injected. For the mRNA rescue experiments, *pk1a* or *vhnf1* mRNA was synthesized from a full-length *pk1a* PCR product using mMessage mMachine (Ambion), after the cDNA had been cloned into pCS2(+), similar to previous studies (Matthews et al., 2004). mRNA was injected at the one-cell stage, using 14 pg mRNA for either, similar to previous.

For the chemical and drug injections, 4 ng of the actin inhibitor cytochalasin D (Sigma) was injected into the yolk of 2 dpf larvae, and for the microtubule inhibitor colchicine (Sigma), 20 pg was injected into the yolk. For the RhoA target inhibitor fasudil (Sigma), 10 ng was injected at the 1 cell stage. 6 ng of the JNK inhibitor dicoumeral (Sigma) was injected at 2 dpf. For the Rho kinase inhibitor H-1152 (RKI, EMD Chemicals), 1 ng was injected at 2 dpf. The above doses were determined based on initial titration experiments, and the volume injected was approximately 2 nl, consistent with standard volumes used in MO injection experiments. For the epistasis experiments, 1 ng cytochalasin D or 5 pg colchicine was used with 0.38 ng MO as noted above.

PED-6 treatment

Control and morpholino-injected larvae at 5 dpf were soaked 2 h in 0.1 μg/ml PED-6, similar to previous studies (Matthews et al., 2004). Larvae were sorted and counted based on gallbladder intensity and location, as indicated in Results. For purposes of quantification, gallbladders were scored as "normal," "faint," "absent," or "left." The distinction between "normal" and "faint" was necessarily subjective, based on the intensity of fluorescence. Larvae for immunostaining were selected from the general pool and not within a particular level of PED-6 uptake. For statistical comparisons, chi-square analysis was performed (http://www.graphpad.com).

Immunostaining and electron microscopy

Whole-mount cytokeratin immunostaining of wild-type and morpholino-injected larvae were performed as previously described (Matthews et al., 2004; Lorent et al., 2004). Briefly, 10–15 larvae per injection round were randomly selected, fixed in 80% MeOH/20% DMSO, peeled, stained with monoclonal antibody Ks18.04 (RDI Division of Fitzgerald Industries) and then stained with appropriate secondary antibody. For electron microscopy, larvae at 5 dpf were fixed, prepared, and examined as previously (Matthews et al., 2009).

Quantification of duct stainings was performed largely similar to previous (Matthews et al., 2004). Total ducts were counted and terminal ductules were counted as previously. "Interconnecting ducts" were defined more strictly for the quantifications presented here, as ducts were considered interconnecting only if both ends clearly terminated in another duct. Duct length was calculated similar to previous, using a Photoshop grid as the unit of length. Lengths are presented with the caveat that they were quantified as two-dimensional images of a three-dimensional structure. Duct angle and width were calculated using ImageJ. Angles were determined by measuring the most acute angle between a main duct and an offshooting duct, and averaging all of the angles within a sample; the angles reported are the means of the averages from each sample. As with duct length, angles may not be the exact angle in a three-dimensional network. Width is reported as mm, based on each sample micrograph as 5 cm × 5 cm and as determined by ImageJ. Numbers depicted represent means ± S.E.M. of 6 samples per condition, with *t*-tests.

PCNA and TUNEL stainings were performed similar to previous (Matthews et al., 2005). Briefly, for PCNA staining, 4 dpf control and *pk1a* MO-injected larvae were stained with αPCNA and 2F11 followed by the appropriate fluorescent secondary antibodies, and livers were examined by confocal microscopy. 2F11-positive cells were examined for concomitant PCNA staining; even faint PCNA staining was counted as positive. For hepatocytes, livers were counterstained with DAPI, and non-2F11-positive cells were counted. While this will count some endothelial cells, hepatocytes greatly outnumber endothelial cells, and we did not count cells with elongated nuclei more typical of endothelial cells. For TUNEL staining, larvae were raised in PTU and then stained using Apoptag (Millipore), similar to previous. We used 0.1N HCl as a positive control, also similar to previous.

Quantitative real-time PCR

Template cDNA was synthesized from RNA obtained from 5 dpf control and *pk1a* MO-injected whole larvae derived from three

independent experiments. Primers for *vhnf1* and *hprt* were previously described (Matthews et al., 2004). Analysis was performed as described previously (Matthews et al., 2004).

Results

Developmental expression of PCP genes in zebrafish liver

We expected PCP genes to be expressed in the liver during the formation of nascent bile ducts, which would support a role for PCP in biliary development. Others have examined PCP gene expression at earlier stages of zebrafish development; in general, PCP expression is diffuse at early stages and then becomes restricted to the developing nervous system (Park and Moon, 2002; Veeman et al., 2003). We examined PCP gene expression at 3 dpf, at which point the bile ducts are beginning to form (Lorent et al., 2004; Matthews et al., 2004). PCP gene expression at these later stages has not previously been examined. As depicted in Fig. 1, our results demonstrated that several PCP genes, including *pk1a, dsh2, vangl2, dsh3, wnt11, wnt11r* and *ankrd6* were expressed in the developing liver at 3dpf. Several other PCP genes, however, such as *pk2* (Fig. 1), *celsr1, celsr2* and *celsr3* (data not shown) were not detectable in the liver at 3 dpf, although we did detect *celsr* expression at earlier stages in the developing nervous system (data not shown). The lack of *celsr* expression in the liver suggests that other genes may occupy this role in the liver, or that PCP functions without *celsr* in the liver. We did not observe expression of these PCP genes in the developing pronephros (Fig. 1), consistent with published expression patterns at earlier stages (http://www.zfin.org). Our expression results support a potential role of PCP in hepatobiliary development.

Knockdown of PCP genes leads to abnormal PED6 uptake and defects in biliary development

To assay the function of PCP genes in zebrafish biliary development, we performed gene knockdown experiments using antisense morpholino oligonucleotides (MOs). Morpholinos were designed to target the 5' translational start site or the splice acceptor site for exon 7 of the *pk1a* gene. Others have previously reported that knockdown of *pk1a* or *pk1b* in zebrafish leads to defects in gastrulation and neuronal migration (Carreira-Barbosa et al., 2003; Rohrschneider et al., 2007; Takeuchi et al., 2003; Veeman et al., 2003), but we used lower MO concentration to avoid effects on gastrulation that would be lethal. We focused our studies on *pk1a*. Fig. S1 demonstrates knockdown after injection at the one-cell stage or at 2 dpf.

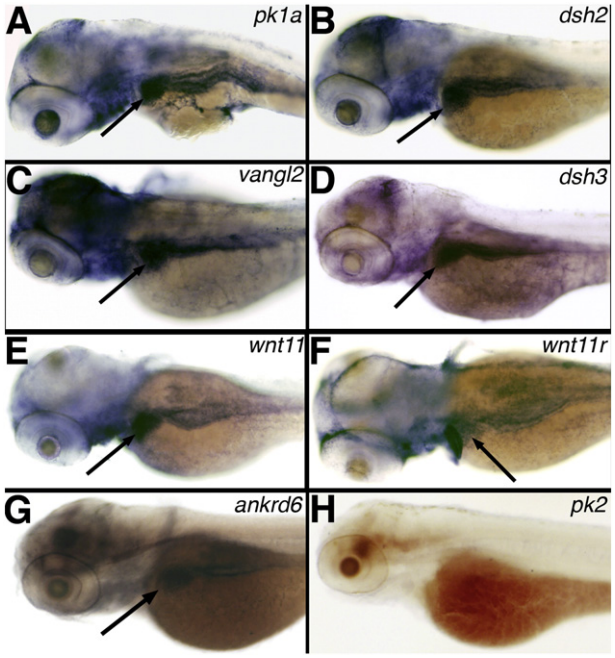

Fig. 1. Expression of PCP genes in 3 dpf zebrafish larvae. Whole-mount RNA in situ hybridization of PCP genes prickle 1a (*pk1a*) (A), dishevelled 2 (*dsh2*) (B), van gogh-like 2 (*vangl2*) (C), dishevelled 3 (*dsh3*) (D), *wnt11* (E), *wnt11r* (F), ankyrin-related domain containing 6 (*ankrd6*) (G), and prickle 2 (*pk2*) (H). Note the liver staining (black arrows) present for A–G, but not in H.

The general morphology of the *pk1a* morphant larvae was preserved, although liver size appeared somewhat reduced (Fig. 2). Gallbladder fluorescence following the ingestion of the quenched fluorescent lipid, PED6 (Farber et al., 2001), was reduced in *pk1a* morpholino-injected larvae (Fig. 2). We classified gallbladder PED6 uptake as "normal" (Fig. 2C), "faint" (Fig. 2D), or "absent" (Fig. 2E), and using this method determined that *pk1a* MO injection resulted in a significant decrease in biliary function (see Supplemental Fig. 2 for breakdown of results, $n=77$ control, 269 morphants, $p<0.0001$). Abnormal gallbladder uptake of PED6 is consistent with defects in intrahepatic biliary development. Thus, these results suggest that PCP defects may lead to defective intrahepatic biliary development. Interestingly, we also observed an increase in left-sided gallbladders in larvae injected with *pk1a* MOs (Fig. 2F and Fig. S2), suggesting that *pk1a* knockdown may affect left-right digestive organ location. Left-sided gallbladders were also of decreased intensity (Fig. 2F). We did not observe gallbladder sidedness defects, although we did observe intensity defects, after *pk1a* morpholino injection at 2 dpf (data not shown), suggesting that the positional defects arise earlier than 2 dpf.

To determine whether *pk1a* knockdown leads to abnormal intrahepatic biliary development, we performed cytokeratin immunostaining of 5 dpf *pk1a* morphants. In zebrafish larvae injected with *pk1a* MO, intrahepatic bile ducts demonstrated abnormal anatomy compared with control (Fig. 2G–I). As also depicted in the schematics in Fig. 2J–L and Table 1, the number of ducts was significantly reduced in the morphant, and there were fewer terminal ductules and interconnecting ducts (ducts that clearly connect one duct with another). The defects observed in cytokeratin immunostaining were also seen in larvae injected with *pk1a* morpholinos at 2 dpf (data not shown). Control MOs included vehicle control, as well as standard and random control MOs; results from all types of negative controls were indistinguishable (Fig. 2 and data not shown). The cytokeratin immunostaining results are thus consistent with the PED6 results and demonstrate that knockdown of *pk1a* perturbs intrahepatic biliary development in zebrafish.

We performed similar knockdown experiments with MOs against *vangl2* and *ankrd6*. As depicted in Fig. 2K–L, knockdown of *vangl2*, which encodes the vertebrate equivalent of the Prickle-binding protein Strabismus, led to a similar pattern of abnormal intrahepatic biliary development, as did knockdown of *ankrd6*, which encodes the vertebrate equivalent of the Prickle antagonist Diego (see Fig. S1 for documentation of knockdown of both *vangl2* and *ankrd6*). Quantitative analysis of duct number and characteristics noted in cytokeratin immunostainings of *pk1a*, *vangl2* and *ankrd6* MO-injected larvae support a similar but milder effect for both *vangl2* and *ankrd6* knockdown (Table 1). Gallbladder PED6 uptake in these morphants also demonstrated abnormally placed left-sided gallbladders (data not shown). These findings suggest that inhibition of the Prickle/Strabismus aspect of PCP leads to developmental biliary defects in zebrafish, and may affect digestive organ localization as well.

Loss of pk1a leads to abnormal localization of digestive organs

As depicted in Fig. 2, there was an increase in the number of left-sided gallbladders in larvae injected with *pk1a* MO. Others have demonstrated that inhibition of PCP activity leads to the failure of the forming gut to migrate to the midline, leading to bilateral expression

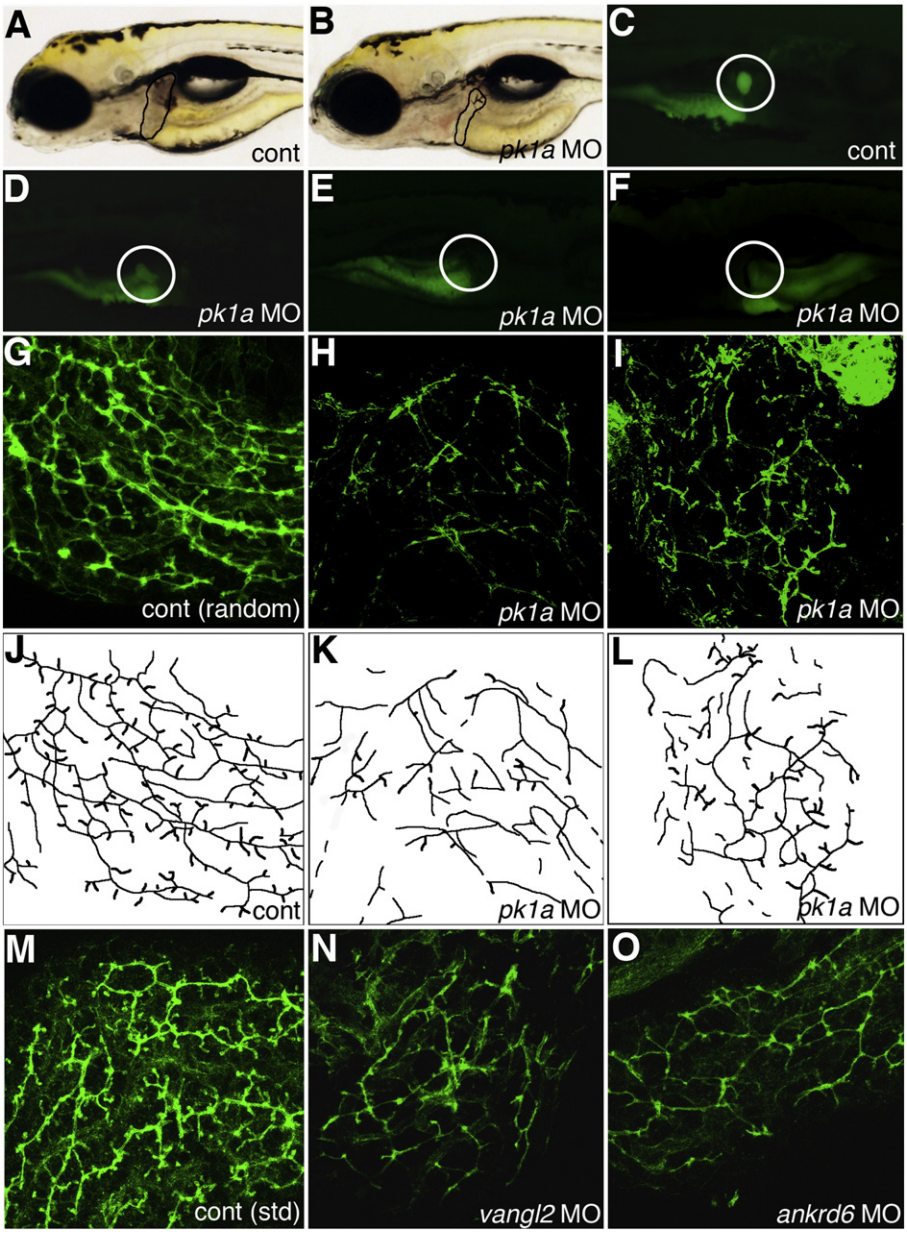

Fig. 2. Altered PED6 gallbladder uptake and bile duct defects in *pk1a* morphants. (A–B) Left lateral view of live 5 dpf control (A, cont) and *pk1a* morpholino-injected (B, *pk1a* MO) larvae. Liver size (black outline) appears smaller in (B), but otherwise the larvae appear similar. (C–F) PED6 uptake in control (C) and three examples of *pk1a* morphants (D–F), showing decreased uptake (D), no uptake (E), and abnormal left-sided placement of the gallbladder (F) in *pk1a* morphants. Note that the view of (C–E) is right lateral and that of (F) is left lateral to show the gallbladder sidedness. (G–I) Confocal projections of whole-mount cytokeratin immunostainings of random control MO-injected (G) and *pk1a* morphant (H, I) livers at 5 dpf demonstrate decreased number and complexity of intrahepatic bile ducts in the *pk1a* morphants. (J–L) Line schematics of ducts in (G–I) to clarify the duct staining pattern. (M–O) Confocal projections of whole-mount cytokeratin immunostainings of livers from 5 dpf larvae injected with standard (std) control MO (M) and larvae injected with MOs against *vangl2* (N) or *ankrd6* (O). Note that the pattern of the ducts in (N) and (O) is similar to the ducts in the *pk1a* MO-injected larva (H, I). Similar results were obtained with either the AUG or splice blocking *pk1a*, *vangl2*, and *ankrd6* MOs.

of various endodermal organ markers at 2 dpf (Matsui et al., 2005). Of note, we did not observe bilateral gallbladders by PED6 uptake in any morphant fish. To determine whether *pk1a* knockdown led to abnormal localization of other digestive organs, we performed in situ hybridizations with digestive organ markers on *pk1a* morphants. In normal 3 dpf zebrafish larvae, the liver and intestine are on the left side, while the pancreas, which contains one islet, and the gallbladder, are on the right side (Wallace and Pack, 2003). As depicted in Fig. 3, expression of the liver gene ceruloplasmin (*cp*) was abnormal in 3 dpf *pk1a* morphants, with a significant number of larvae showing the liver extending from the left side over the midline, a bilateral liver, or a liver on the right side. We observed similar defects in position of the intestine as well as both the exocrine and endocrine pancreas (Supplemental Figs 3–5). Our results are consistent with the previous results of Matsui et al., but further demonstrate that by later time points, the early mislocalization of developing digestive organs may result in abnormal localization of more mature forms of these organs. More recent studies have demonstrated the importance of PCP in establishing left-right asymmetry (Antic et al., 2010; Song et al., 2010), but our results showing occasional "extended" marker staining out from the midline seem more consistent with migration defects.

Forced expression of pk1a leads to abnormal biliary development

To ensure that the abnormal intrahepatic biliary development noted in *pk1a* morphants is specific to *pk1a* MO injection and not a

Table 1
Quantification of bile duct defects in *pk1a*, *vangl2*, and *ankrd6* morpholino-injected larvae. Total numbers of ducts, interconnecting ducts (IC), and terminal ductules are depicted in control, *pk1a*, *vangl2* and *ankrd6* MO-injected larvae. Also depicted are average duct length, width, and angles between branching ducts. Length is based on grids in Photoshop, while width is measured as mm from a 5 cm × 5 cm image. Angles refer to the average angle at which ducts grow out from other ducts, measuring the most acute angle; there was considerable variability within samples but the average angles were remarkably consistent. $^{*}p<0.05$, $^{**}p<0.005$, $^{***}p<0.0005$. Values without asterisks are not significantly different from control. $n=6$ per condition, ±S.D.

Condition	No. of ducts	No. of IC ducts	No. of terminal ductules	Duct length	Duct width	Duct angles
Control	50.2 ± 5.7	16.8 ± 5.0	84.7 ± 17.4	1.64 ± 0.22	0.413 ± 0.053	80.2 ± 3.7
pk1a	MO 21.5 ± 11.1***	1.3 ± 0.8***	16.8 ± 6.9***	1.20 ± 0.30*	0.401 ± 0.056	71.0 ± 4.2*
vangl2 MO	20.5 ± 2.9***	3.2 ± 2.1***	15.0 ± 9.7***	1.55 ± 0.58	0.357 ± 0.038	76.8 ± 4.3
ankrd6 MO	24.2 ± 10.3***	5.2 ± 5.0**	20.2 ± 8.2***	1.38 ± 0.35	0.379 ± 0.028	76.7 ± 4.3

result of off-target knockdown or developmental delay, we co-injected *pk1a* MO with *pk1a* mRNA. As depicted in Fig. 4, co-injection of MO and mRNA led to normalization of both PED6 gallbladder intensity and sidedness, suggesting that both effects are due to specific inhibition of Pk1a activity in the *pk1a* morphants. Fig. 4A further suggests that *pk1a* mRNA injection alone may have a modest effect on biliary development, as gallbladder intensity is decreased in larvae injected with *pk1a* mRNA. Interestingly, forced expression of *pk1a* mRNA did not appear to affect gallbladder left-right sidedness, although injection of the mRNA with the morpholino did appear to rescue that aspect of the phenotype. Cytokeratin immunostaining of liver from 5 dpf larvae injected with *pk1a* mRNA demonstrated abnormal intrahepatic biliary anatomy (Fig. 4D), suggesting that forced expression of *pk1a* perturbs intrahepatic biliary development. Furthermore, co-injection of *pk1a* morpholino and mRNA led to normalization of the phenotype (Fig. 4E). These results demonstrate that the effect of *pk1a* knockdown on biliary development is specific, and also suggest that forced expression of *pk1a* leads to defects in biliary development. The differential effects of *pk1a* mRNA injection on gallbladder sidedness vs. intrahepatic biliary defects suggest that these phenotypes may result from separate mechanisms of Prickle action.

Cellular defects in pk1a morphants

Defects in intrahepatic biliary development may be caused by global defects in the liver affecting both the developing hepatocytes and bile duct cells, or by defects specifically affecting either the developing hepatocytes or bile duct cells. The expression studies in Fig. 1 suggested that *pk1a* is expressed throughout the liver, or possibly only in the larger and more prevalent hepatocytes. To further elucidate the developmental biliary defects in *pk1a* morphants, we examined biliary cells in the morpholino-injected larvae using the marker 2F11, which stains bile duct cells (Crosnier et al., 2005). Fig. 5 demonstrates that 2F11 staining showed fewer bile duct cells and less extensive projections to neighboring cells, consistent with the cytokeratin staining demonstrating fewer and less complex ducts.

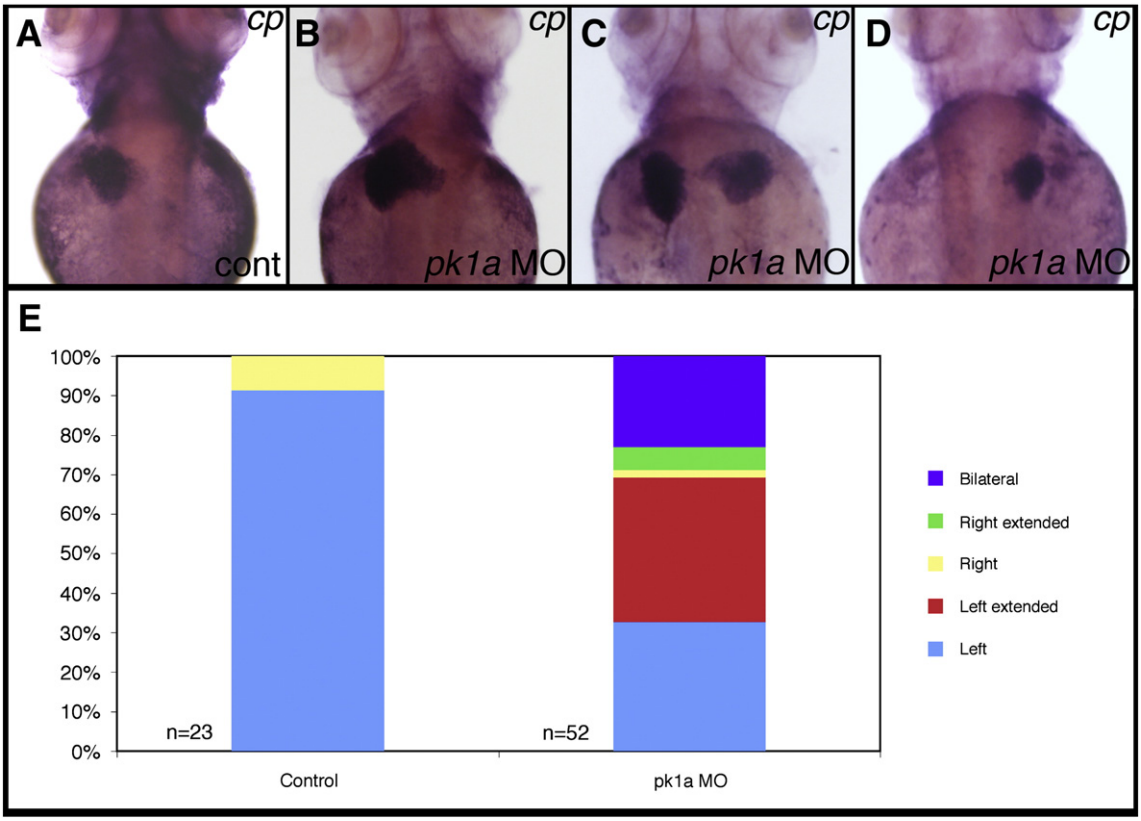

Fig. 3. Abnormal liver localization in *pk1a* morphants. Whole-mount in situ hybridization of ceruloplasmin (*cp*), a liver marker, in 3 dpf *pk1a* morphants demonstrates abnormal liver location, including "right extended" (B), "bilateral" (C), and "right" (D). (E) Graph depicting the scoring of *pk1a* morphants demonstrates a significant difference in the total number of abnormally localized livers (9% vs. 67%, $p<0.0001$ by chi-square test), while the difference in livers limited to the right side is not significant (9% vs. 8%). Please see supplemental data for localization defects in other organs.

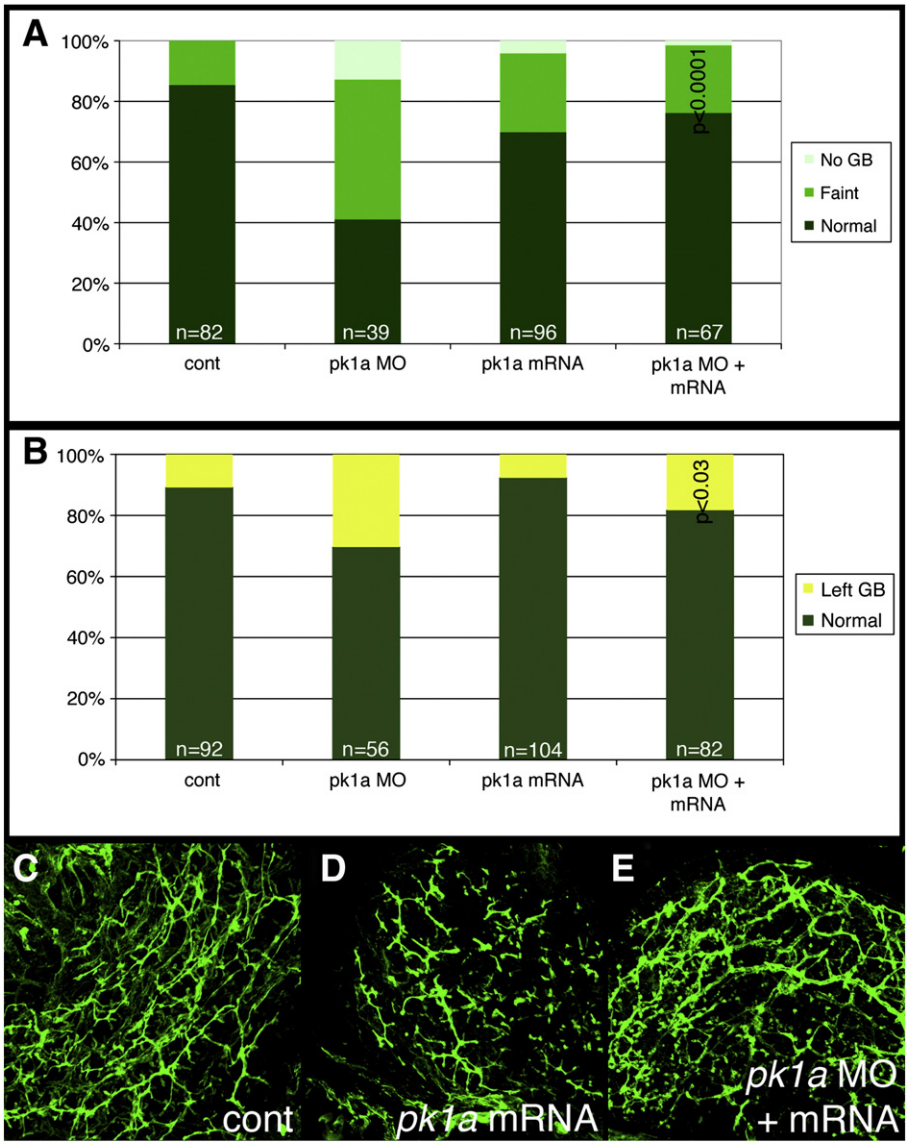

Fig. 4. Effect of *pk1a* on biliary development. (A, B) Bar graphs depicting PED6 uptake in control (cont), *pk1a* morpholino-injected (pk1a MO), *pk1a* mRNA-injected, and *pk1a* MO and mRNA-injected larvae. In (A), the percentage of larvae with no gallbladder (GB) uptake, faint uptake, and normal uptake is depicted on the *Y*-axis. In (B), numbers of larvae with abnormal left-sided GBs are depicted. Note that *pk1a* mRNA injection leads to an increase in the number of faint gallbladders compared to control ($p<0.0001$), while mRNA injection leads to a rescue of the MO phenotype ($p<0.0001$ compared to MO injection, NS compared to control). Forced expression of *pk1a* mRNA has no effect on GB sidedness, but does rescue the morphant sidedness phenotype. (C–E) Confocal projections of whole-mount cytokeratin staining of livers from 5 dpf control (B, cont), *pk1a* mRNA-injected (C) and *pk1a* MO and mRNA injection (D). Note that mRNA injection alone leads to scattered short duct-like structures, while mRNA and MO co-injection leads to rescue of the MO phenotype.

As depicted in Fig. 5 and Table 2, there were fewer bile duct cells in the morphants, as determined by 2F11 and DAPI costaining; there were fewer hepatocytes as well, but the proportion of bile duct cells is decreased in the morphants, suggesting that the effect may be more severe in bile ducts.

To determine whether the changes in biliary cell number were due to increased cell death or decreased cell division, we examined *pk1a* morphant larvae stained with TUNEL or PCNA. There was no apoptotic cell death appreciated in *pk1a* morphant or control larvae (data not shown), but Fig. 5 and Table 3 demonstrate that there was significantly less bile duct cell proliferation in 4 dpf *pk1a* morphant larvae, while hepatocyte proliferation was similar to control. In contrast to the results of 5 dpf larvae in Table 2, at 4 dpf there appear to be similar numbers of hepatocytes, possibly because of slower growth in the morphants that is manifested at 5 dpf. The decrease in bile duct cell proliferation most likely leads to the decreased number of bile duct cells observed in the morphants. The decreased number of bile duct cells likely plays a role in the biliary developmental defects.

To more closely examine the hepatocytes and bile duct cells in the *pk1a* morphants, we examined tissue sections. There was no appreciable difference in the appearance of liver sections in control and *pk1a* MO-injected larvae by hematoxylin and eosin staining (data not shown). Given the lack of a lobular structure and portal triads in teleost larvae and adults (Hinton and Couch, 1998), differences may be more difficult to appreciate by this method, however. Thus, we examined larvae by electron microscopy. As depicted in Fig. 5E–F, lower magnification views demonstrated generally preserved morphology, although there appeared to be an accumulation of vesicles in hepatocytes near canaliculi, and bile within the ducts appeared abnormal (Fig. 5F). Higher magnification views of bile duct cells demonstrated abnormal-appearing Golgi and accumulation of intracellular vesicles (Fig. 5G–H). The phenotypic distinction between hepatocytes and bile duct cells evident in both controls and morphants suggests that the defects after *pk1a* knockdown are probably not related to defects in differentiation, as that would be expected to lead to a more homogeneous population of cells in the

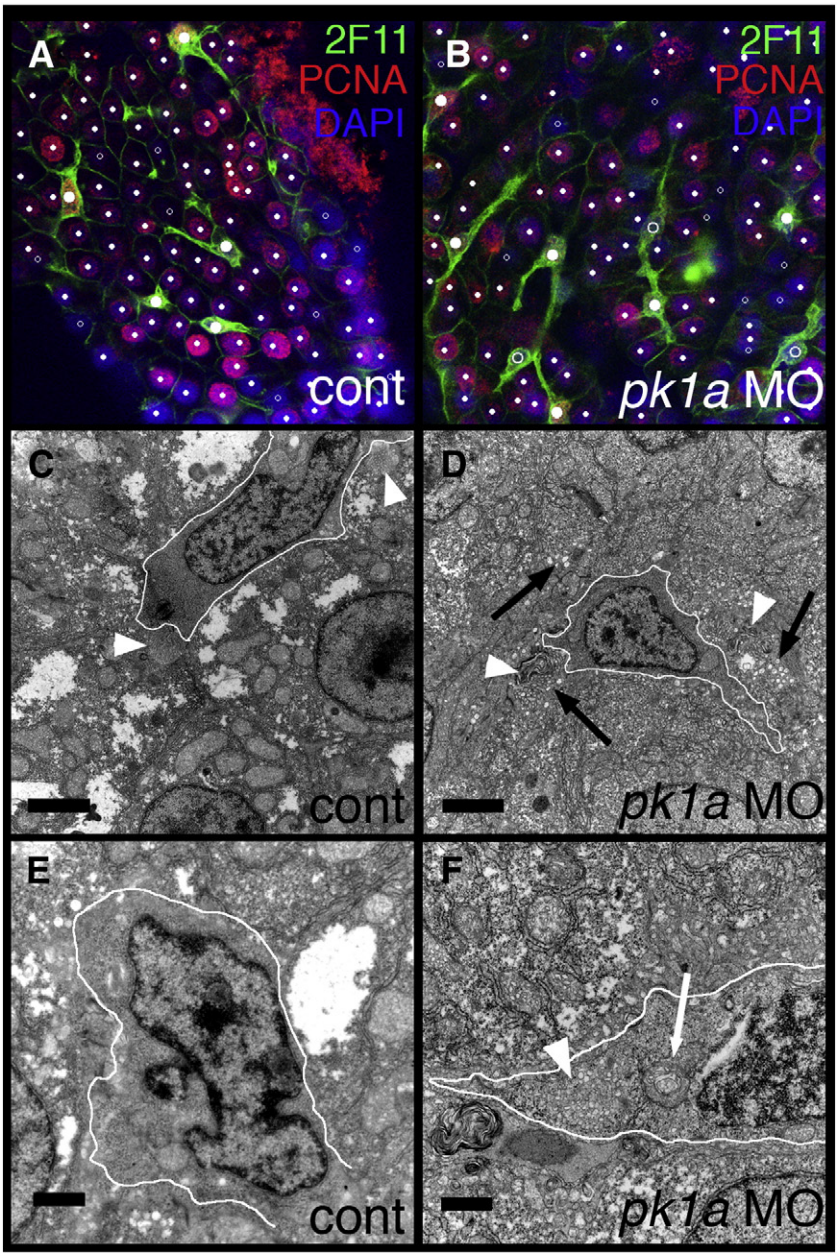

Fig. 5. Abnormal bile duct cells in *pk1a* morphant livers. (A–B) Single confocal optical slices of whole-mount 2F11 and PCNA immunostaining of livers from 5 dpf control (A, cont) and *pk1a* morphant (B) larvae. 2F11 staining is in green, PCNA in red, and DAPI counterstain in blue. Hepatocytes are noted with small white dots, while biliary cells are noted with larger dots. Solid dots represent cells that are PCNA positive, while the open dots are PCNA negative. Note that the biliary cells in control are all PCNA positive, while there are PCNA negative biliary cells in the *pk1a* morphant. (C-F) Electron micrographs from livers from control (C, E, cont) and *pk1a* morpholino-injected (D, F, *pk1a* MO) larvae. (C–D) Low power views (scale bar 2 μm) demonstrate overall similarity in appearance, but canaliculi (white arrowheads) appear to have accumulated material within in the morphants (D), and there is an accumulation of vesicles (black arrows) in the hepatocytes in (D). (E–F) Higher power views (scale bar 500 nm) demonstrate dilated Golgi (white arrow) in the bile duct cell in the morphant sample (F), as well as an accumulation of intracellular vesicles (F, white arrowhead). The white outlines circumscribe the bile duct cells in C–F.

Table 2
Numbers of biliary cells in *pk1a* morphants. Confocal projections of 2F11 immunostaining of livers from control and *pk1a* MO-injected 5 dpf larvae were assayed for total cell number (by DAPI staining) and bile duct cell (BDC) number (by 2F11 and DAPI). The total cell number is lower in the morphants, but the number of bile duct cells is lower than would be expected. Means represent average of 5 samples, ± S.D.

	Total cells	Bile duct cells	%BDC
Control	562.4 ± 37.9	58.0 ± 7.0	10.3 ± 1.0
pk1a MO	371.2 ± 115.0	30.6 ± 9.2	8.3 ± 1.0
	$p<0.03$	$p<0.001$	$p<0.03$

morphant liver. The accumulation of vesicles is consistent with defects in intracellular trafficking, although these vesicles could be secondary to poor bile flow and resulting impaired transport to the canalicular membrane. These results suggest that *pk1a* knockdown affects both hepatocytes and bile duct cells, although the greater effect on bile duct cell number noted above suggests that the effects on bile duct cells may be more severe.

Inhibition of downstream PCP targets also leads to biliary defects

PCP family members have been shown to exert effects via RhoA and Rho kinase (Strutt et al., 1997), and c-Jun N-terminal kinase (JNK) (Yamanaka et al., 2002). Therefore, we examined whether inhibition of

Table 3
Decreased bile duct cell proliferation in *pk1a* morphants. Bile duct cells (BDCs) and hepatocytes from livers from 4 dpf control and *pk1a* MO-injected larvae were assayed for cell proliferation, using PCNA to label proliferating cells and 2F11 to label BDCs. There is a significant reduction in proliferating BDCs in the morphants, as an absolute number and as a percentage of the total number of BDCs. There is no difference in the number of proliferating hepatocytes. Means represent an average of 5 samples, ±S.D. Similar results were obtained with either *pk1a* MO.

	No. of BDCs	No. of BDCs with PCNA	% Proliferating
Control	28.8 ± 2.8	26.2 ± 2.3	91.1 ± 3.7
pk1a MO	24.2 ± 5.6	18.4 ± 3.8	76.6 ± 7.0
	p = N.S.	p<0.005	p<0.005
	No. of hepatocytes	No. of hepatocytes with PCNA	% Proliferating
Control	151.8 ± 29.8	133.3 ± 21.7	88.3 ± 3.9
pk1a MO	150.8 ± 29.9	130.7 ± 32.4	86.0 ± 4.6
	p = N.S.	p = N.S.	p = N.S.

Rho kinase or JNK affected biliary development. As depicted in Fig. 6 and Table 4, intrahepatic biliary anatomy was abnormal at 5 dpf in larvae treated with the Rho kinase inhibitors fasudil (Tamura et al., 2005) and H-1152 (RKI) (Ikenoya et al., 2002), and after treatment with the JNK inhibitor dicoumeral (Cross et al., 1999). There is phenotypic similarity between intrahepatic bile ducts in *pk1a* morphants and larvae treated with the Rho kinase inhibitors, with fewer and shorter ducts (Figs. 6 and S6, Table 4). Ducts from larvae treated with the JNK inhibitor appear more severely affected, however, suggesting that JNK inhibition may overlap with other pathways in addition to PCP. These results do support a role for PCP in biliary development, though, as inhibition of Rho kinase or JNK negatively affects intrahepatic biliary development, consistent with involvement of pathways downstream of PCP in zebrafish biliary development.

Rho kinase and JNK exert effects on the cytoskeleton, affecting both the actin and microtubule cytoskeletons (Ciani et al., 2004; Takeuchi et al., 2003). We examined biliary development after treatment with the actin inhibitor cytochalasin D or the microtubule inhibitor colchicine to determine whether inhibition of cytoskeletal components could affect biliary development. As depicted in Fig. 6 (as well as Table 4 and Fig. S6), treatment with either cytochalasin D or colchicine led to abnormal biliary development, similar to Rho kinase inhibition and to knockdown of *pk1a*, but milder than JNK inhibition. To determine whether PCP inhibition and the colchicine or cytochalasin D effects were epistatic, we injected *pk1a* MOs and cytochalasin D or colchicine at doses that alone resulted in no or only mild effects. As demonstrated in Fig. 6, while there was no effect of these treatments alone on gallbladder PED6 uptake in the larvae, when combined there was a significant reduction in gallbladder intensity. Cytokeratin immunofluorescence was abnormal only in the livers from larvae treated with both the *pk1a* MO and colchicine or cytochalasin D in low doses (Fig. 6), as expected from the results with PED6. These results suggest that the biliary defects noted from PCP gene knockdown may be mediated via effects on the cytoskeleton, as would be expected given previous results on downstream targets of PCP.

pk1a and hnf6 knockdown are synergistic

The appearance of the developmental defects in *pk1a* morphants and in larvae injected with *pk1a* mRNA was similar to the pattern observed with knockdown and forced expression of *hnf6*, and similar to *vhnf1* mutants (Matthews et al., 2004). Thus, we examined expression of *vhnf1*, a downstream target of *hnf6*, in *pk1a* morphants. *vhnf1* expression was decreased in *pk1a* morphants, as determined by quantitative PCR normalizing to *hprt* (Fig. 7) and liver-specific *cp* (data not shown). In situ hybridization also demonstrated a decrease in liver expression of *vhnf1* (Fig. 7), while expression of *cp* appeared relatively constant, regardless of the placement of the liver (Fig. S7). These results are consistent with *pk1a* acting upstream of *vhnf1*. Similar to the experiments described above, we injected *pk1a* and *hnf6* MOs at lower doses singly and in combination to determine whether inhibition of these genes worked synergistically, suggesting that the two gene products work in the same pathway. As depicted in Fig. 7 and quantified in Table 5, only knockdown of both genes led to decreased PED6 gallbladder uptake and abnormal cytokeratin immunostaining, suggesting that *pk1a* and *hnf6* are operating in the same pathway. This overlap likely at least includes effects on *vhnf1* but may also involve additional effects. Interestingly, injection of *hnf6* MO did not seem to affect gallbladder sidedness (data not shown), suggesting that the effect of *hnf6* is on intrahepatic biliary morphogenesis only. Consistent with this, injection of *vhnf1* mRNA into *pk1a* morphants led to rescue of gallbladder PED6 intensity but not sidedness, and improved the appearance of *pk1a* MO-injected intrahepatic bile ducts (Fig. 7 and Table 5). Injection of *vhnf1* mRNA led to rescue of the *pk1a* morphant biliary phenotype after injection of *pk1a* MO at the 1-cell stage (Fig. 7 and Table 5) or at 2 dpf (data not shown). Interestingly, *vhnf1* injection did not rescue the decrease in duct angle, suggesting that directional duct outgrowth may not be dependent on *vhnf1*, although there was considerable variability in duct angle within samples. These results suggest that *pk1a, hnf6* and *vhnf1* function in the same genetic pathway in zebrafish intrahepatic biliary development, and that forced expression of *vhnf1* rescues PCP defects caused by *pk1a* knockdown.

Discussion

One in 3000 infants develops hepatobiliary disease leading to poor bile flow within the first few months of life. Among the less common causes of infantile hepatobiliary diseases are disorders in which patients also develop kidney cysts, although some of these disorders may also manifest later in life as well. Recently, abnormalities in PCP signaling were found to be associated with kidney cysts. Here, we present data from zebrafish that support an importance of PCP signaling in hepatobiliary development. Multiple PCP members were expressed in the liver during biliary development. Morpholino antisense-mediated knockdown of *pk1a* and other PCP genes demonstrated impaired bile duct formation, and we also observed defects in left–right location of multiple digestive organs. We have presented additional evidence supporting a role for PCP in biliary development, as inhibition of known downstream targets of PCP such as Rho kinase, JNK, and cytoskeletal components also led to biliary defects. Finally, we demonstrated that these effects are in the same pathway as *hnf6* and *vhnf1* – transcription factors important in biliary development.

Importance of PCP in biliary development

Examination of PCP in vertebrates has demonstrated a role for PCP in early developmental phenomena such as gastrulation (Takeuchi et al.,

Fig. 6. Inhibition of Rho kinase, JNK, and cytoskeletal architecture negatively affects biliary development. (A–F) Whole-mount projections of cytokeratin immunostaining of liver from a 5 dpf control larvae (A), compared to similar stainings from larvae treated with the Rho kinase inhibitors fasudil (B) and H-1152 (RKI, C), as well as the JNK inhibitor dicoumeral (D), the actin inhibitor cytochalasin D (E), and the microtubule and cytoskeleton inhibitor colchicine (F). Note that inhibition of any of the above downstream targets of PCP leads to a phenotype similar to the *pk1a* morphant phenotype. (G) Bar graph depicting PED6 treatment of control larvae compared to larvae treated with low dose *pk1a* morpholino, low dose cytochalasin D, or the combination. Note that alone, the low dose MO or cytochalasin have no to minimal effect, but that in combination, the effect is sizable and significant (p<0.0005, chi-square). (H) Bar graph depicting PED6 treatment of control larvae compared to larvae treated with low dose *pk1a* morpholino, low dose colchicine, or the combination. Note that only in the combination is there a statistically significant effect on PED6 gallbladder uptake (p<0.0001, chi-square test). (I–N) Confocal projections of cytokeratin immunostaining of livers from 5 dpf control larvae (I) and larvae injected with low dose (l.d.) *pk1a* MO (J), low dose cytochalasin D (cyto D, K), low dose colchicine (colch, L), and low dose *pk1a* MO with low dose cytochalasin D (M) or low dose colchicine (N). Note that (J–L) appear similar to control (I), but that (M, N) are abnormal.

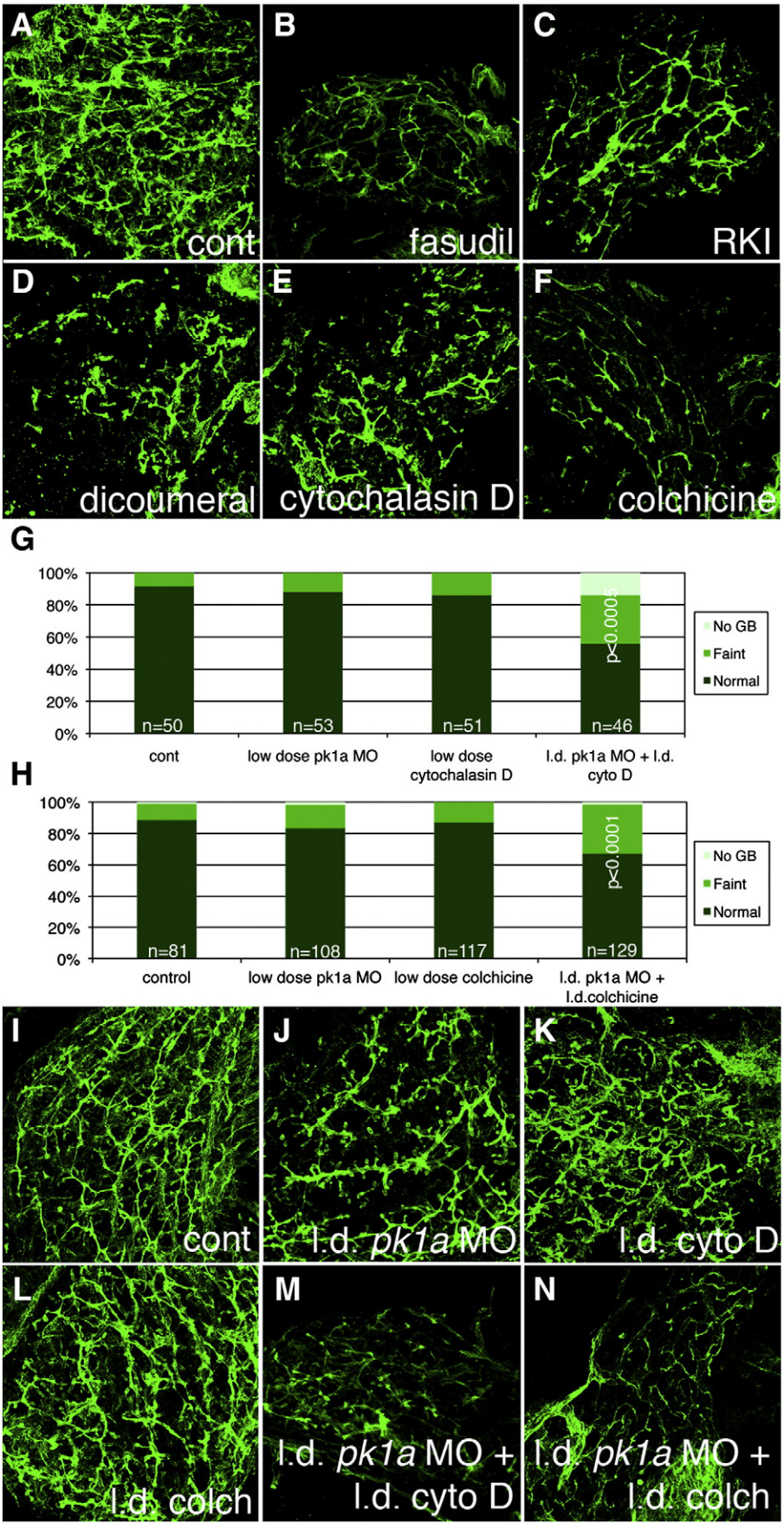
A
cont
B
fasudil
C
RKI
D
dicoumeral
E
cytochalasin D
F
colchicine
G
100%
80%
60%
40%
20%
0%
n=50
n=53
n=51
n=46
p<0.0005
No GB
Faint
Normal
cont
low dose pk1a MO
low dose cytochalasin D
l.d. pk1a MO + l.d. cyto D
H
100%
80%
60%
40%
20%
0%
n=81
n=108
n=117
n=129
p<0.0001
No GB
Faint
Normal
control
low dose pk1a MO
low dose colchicine
l.d. pk1a MO + l.d.colchicine
I
cont
J
l.d. pk1a MO
K
l.d. cyto D
L
l.d. colch
M
l.d. pk1a MO + l.d. cyto D
N
l.d. pk1a MO + l.d. colch

Table 4
Quantification of bile duct defects in larvae treated with various chemical inhibitors. Total numbers of ducts, interconnecting ducts (IC), and terminal ductules are depicted in control, fasudil-, RKI-, dicoumeral-, colchicine-, and cytochalasin D-treated larvae. Also depicted are average duct length, width, and angles between branching ducts. Length is based on grids in Photoshop, while width is based on mm from a 5 cm × 5 cm image. $^{*}p<0.05$, $^{**}p<0.005$, $^{***}p<0.0005$. Values without asterisks are not significantly different from control. $n=6$ per condition, ±S.D.

Condition	No. of ducts	No. of IC ducts	No. of terminal ductules	Duct length	Duct width	Duct angles
Control	50.2 ± 5.7	16.8 ± 5.0	84.7 ± 17.4	1.64 ± 0.22	0.413 ± 0.053	80.2 ± 3.7
Fasudil	27.2 ± 10.8**	3.5 ± 3.2***	22.3 ± 5.7***	1.11 ± 0.27**	0.363 ± 0.038	73.0 ± 4.2*
RKI	28.7 ± 11.4**	5.8 ± 4.2**	31.2 ± 8.4***	1.59 ± 0.56	0.411 ± 0.048	78.7 ± 7.0
Dicoumeral	22.7 ± 4.6***	0.2 ± 0.4***	11.3 ± 7.3***	1.14 ± 0.35*	0.531 ± 0.114*	78.6 ± 6.8
Colchicine	32.0 ± 14.8*	3.2 ± 2.9***	15.5 ± 11.1***	1.13 ± 0.35*	0.411 ± 0.076	72.0 ± 4.4*
Cytochalasin	29.7 ± 12.7**	1.8 ± 1.5***	24.0 ± 24.7**	1.20 ± 0.35*	0.424 ± 0.064	77.0 ± 8.6

2003; Veeman et al., 2003; Wallingford et al., 2000) and neurulation (Wang et al., 2006), as well as in later phenomena such as neurite outgrowth (Okuda et al., 2007) establishment of the neuromuscular junction (Jing et al., 2009), cochlear development (Wang et al., 2005), and the renal collecting system (Fischer et al., 2006; Saburi et al., 2008). In many of these examples, there is directionality in cell growth; e.g., the renal collecting system elongates in one direction. PCP proteins may be acting as cues dictating the direction in which cellular proliferation and/or movement occur during growth and development.

A role for PCP in mediating cell proliferation and movement in intrahepatic biliary differentiation seems plausible. In zebrafish, intrahepatic ducts appear by 60 hpf, and over the next several days the ducts lengthen, although new bile duct cells continue to appear (Lorent et al., 2010; Lorent et al., 2004). Branching and interconnecting

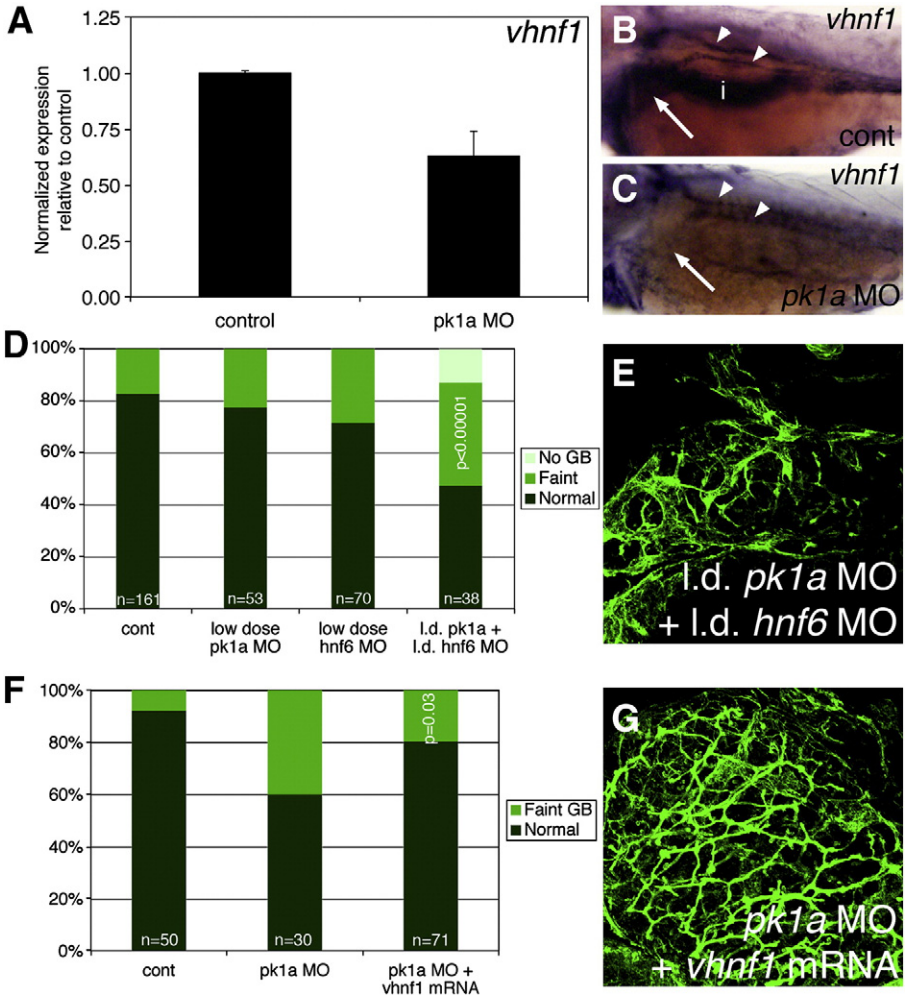

Fig. 7. *hnf6* and *vhnf1* act downstream of PCP in zebrafish biliary development. (A) Quantitative real-time PCR of *vhnf1* expression in control and *pk1a* MO-injected larvae demonstrating a 40% decrease in *vhnf1* expression in the morphants. (B, C) In situ hybridizations of 3 dpf control (B, cont) and *pk1a* MO-injected larvae (C) showing expression of *vhnf1* in pronephric ducts in both conditions (white arrowheads), but no expression in the morphant liver (white arrow) or intestine (i). (D) Epistasis experiment demonstrating that knockdown of *pk1a* and *hnf6* is synergistic with respect to an effect on gallbladder PED6 intensity. (E) Confocal projection of cytokeratin immunostaining of livers from 5 dpf larvae injected with the combination of low dose *pk1a* and *hnf6* MOs, showing a pattern of intrahepatic bile ducts similar to that seen after knockdown of *pk1a*, seen elsewhere. (F) Similar graph of PED6 gallbladder intensity for rescue of *pk1a* knockdown phenotype by *vhnf1* mRNA injection demonstrating improvement in gallbladder intensity ($p=0.03$). (G) Confocal projection of cytokeratin immunostaining of livers from 5 dpf larvae injected with *pk1a* MO with *vhnf1* mRNA, demonstrating a pattern similar to control, seen elsewhere.

Table 5
Quantification of bile duct defects in larvae treated with *pk1a* MO-injection and *hnf6* MO or *vhnf1* RNA injection. Total numbers of ducts, interconnecting ducts (IC), and terminal ductules are depicted in control larvae, and larvae injected with *pk1a* MO, low dose (ld) *pk1a* MO and low dose *hnf6* MO, and *pk1a* MO plus *vhnf1* mRNA. Also depicted are average duct length, width, and angles between branching ducts. Length is based on grids in Photoshop, while width is based on mm from a 5 cm × 5 cm image. $^{*}p<0.05$, $^{**}p<0.005$, $^{***}p<0.0005$. Values without asterisks are not significantly different from control. $n=6$ per condition, ±S.D.

Condition	No. of ducts	No. of IC ducts	No. of terminal ductules	Duct length	Duct width	Duct angles
Control	50.2 ± 5.7	16.8 ± 5.0	84.7 ± 17.4	1.64 ± 0.22	0.413 ± 0.053	80.2 ± 3.7
pk1a MO	21.5 ± 11.1***	1.3 ± 0.8***	16.8 ± 6.9***	1.20 ± 0.30*	0.401 ± 0.056	71.0 ± 6.9*
ld *pk1a* MO + ld *hnf6* MO	18.0 ± 9.8***	0.7 ± 0.8***	26.2 ± 21.0***	1.34 ± 0.53	0.374 ± 0.010	73.6 ± 3.4*
pk1a MO + *vhnf1* mRNA	37.7 ± 11.0*	14.0 ± 4.6	94.2 ± 28.9	1.98 ± 0.27*	0.408 ± 0.071	73.3 ± 4.5*

occur in the later stages of biliary development (Matthews et al., 2004). Intrahepatic bile ducts in the *pk1a* MO-injected, Rho kinase or cytoskeletal inhibitor-treated larvae have fewer and shorter ducts than control larvae, and resemble the intrahepatic ductal pattern of a 3 dpf larva. There are fewer bile duct cells in *pk1a* morphants, most likely from a decrease in cell proliferation. Decreased cell proliferation has been observed previously in other models after inhibition of PCP activity, notably in angiogenesis (Cirone et al., 2008), a process that appears similar to intrahepatic biliary development in zebrafish. Thus, our results in zebrafish are consistent with a model in which PCP family members are important in bile duct cell proliferation, affecting intrahepatic duct proliferation and lengthening, similar to the role of PCP family members in other systems. In mammals, intrahepatic biliary development proceeds out towards the periphery of the liver (Roskams and Desmet, 2008); PCP proteins could be involved in duct lengthening in mammals as well.

We also provide evidence that PCP inhibition leads to a decrease in the expression of *vhnf1*, a homeodomain transcription factor downstream of *hnf6* that is important in biliary development in mammals (Clotman et al., 2002; Coffinier et al., 2002) and zebrafish (Matthews et al., 2004). Zebrafish *vhnf1* mutants not only demonstrate biliary defects (Matthews et al., 2004), but kidney cysts as well (Sun and Hopkins, 2001). More recent evidence demonstrates that *vhnf1* is also critical for early stages of liver specification in both mammals and zebrafish (Lokmane et al., 2008). Our results suggest that the effect of PCP on *vhnf1* may be more important in the later stages, in which *vhnf1* plays a role in biliary development, as *pk1a* knockdown does not result in complete lack of liver formation. Moreover, *vhnf1* mRNA injection rescued biliary defects in both early and late MO-mediated inhibition of *pk1a*, supporting a role for *pk1a* in the later effects of *vhnf1* on biliary development. Whether *vhnf1* expression is affected by Pk1a directly or indirectly is as yet unclear, but the possibility of a direct mediation of Hnf6 or *vhnf1* gene expression by PCP is intriguing.

The combination of effects of PCP on biliary development, involving effects on cell proliferation, intracellular trafficking, and *hnf6*/*vhnf1* activity suggests a possible role for TGFβ signaling. PCP defects could result in impaired trafficking of TGFβ or its receptor, both of which have been shown to be important for TGFβ signaling (Le Roy and Wrana, 2005; Roth-Eichhorn et al., 1998). TGFβ activity leads to increased liver cell proliferation (Fausto et al., 1995), is activated in differentiation of hepatoblasts into biliary cells (Ader et al., 2006), and is involved in a complex regulatory pathway with Hnf6 in mediating biliary development (Clotman et al., 2005). Pk1a has been shown to interact with several other proteins, including transcription factors (Shimojo and Hersh, 2003), and thus the effect on *hnf6* or *vhnf1* could also be mediated through an interaction with a transcription factor that binds both Pk1a and the *hnf6* or *vhnf1* promoter. The mechanism of PCP inhibition on biliary development may be due to one or more of the above effects.

Importance of PCP in digestive organ localization

We demonstrated an increase in the number of abnormally sided gallbladders in larvae injected with *pk1a* MOs. Furthermore, we showed that knockdown of *pk1a* led to abnormal distribution of endodermal tissue markers with respect to the left–right body axis, suggesting that inhibition of PCP activity is associated with formation of intestine, liver and pancreas on either or both sides of this axis. Our digestive marker stainings were not always discretely localized to one side or the other, as they occasionally demonstrated extension from the midline to the left or right. These results are consistent with previous results demonstrating bilateral localization of normally asymmetrically localized endodermal tissues at earlier stages (Matsui et al., 2005). We cannot exclude a role for early left–right cues, as recently shown for PCP genes *Vang1* and *Pk2* in mice and Xenopus (Antic et al., 2010; Song et al., 2010), but the presence of the "extended" digestive markers seems more consistent with a migration defect.

Matsui et al. demonstrated that inhibition of PCP activity leads to persistence of endodermal cells lateral to the developing gut tube, suggesting that PCP activity is necessary for successful migration of these cells to the midline. In zebrafish, endodermally derived organs such as the liver and pancreas may develop from tissue surrounding the nascent gut tube (Wallace and Pack, 2003), or from the developing gut tube itself (Field et al., 2003a; Field et al., 2003b). Our data are compatible with both models, as inhibition of PCP activity may lead to ectopic development of pancreas and liver because of a failure of the developing gut tube to become restricted to the midline. Inhibition of PCP activity may also inhibit lateral movement of cells in developing endodermal organs to the correct side, resulting in the persistent expression of markers extending from the midline. Regardless, our results corroborate those of Matsui et al. proposing a role for PCP activity in directional cell migration during endodermal development. The effect of PCP inhibition on digestive development thus appears to lead to abnormally formed tissues that may also end up with abnormal left–right placement, which is most strongly supported by our results showing abnormal biliary development and left-sided gallbladder.

The constellation of left–right digestive organ localization defects, biliary defects, and kidney cysts is found in various combinations in several clinical conditions, including both rare disorders and more common conditions such as autosomal recessive polycystic kidney disease and syndromic biliary atresia (Maclean and Dunwoodie, 2004). Examination of genetic etiologies of these conditions has focused on early left–right asymmetry genes and cilia genes, but recent work implicates PCP in at least some of these conditions (Bacallao and McNeill, 2009; Kim et al., 2010). Although a direct connection between PCP core proteins and ciliogenesis in mammals is not evident, several studies have shown a functional interaction between PCP processes and cilia (Ferrante et al., 2009; Gray et al., 2009; Heydeck et al., 2009; Maisonneuve et al., 2009; Mitchell et al., 2009; Ross et al., 2005), suggesting that defects in these pathways could lead to similar phenotypes. Thus, it would seem likely that defects in PCP would lead to developmental biliary defects and associated clinical findings such as left–right anomalies, both in vertebrate models and possibly in patients as well.

PCP as one of several pathways involved in biliary development

We have presented evidence that inhibition of PCP negatively affects biliary development in zebrafish. This is a previously undescribed role

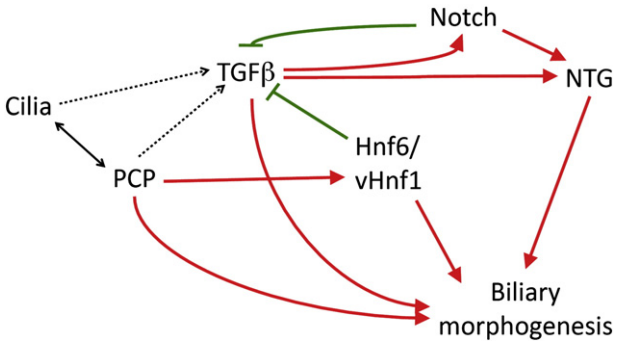

Fig. 8. Schematic pathway interactions in biliary development. Depicted is a schematic of various pathways known to be important in biliary development and the relationship between each pathway. Positive regulation is noted by red arrows, negative by green. Most relationships depicted are based on previous studies; our studies presented here on PCP are included. Possible or unclear relationships are noted with dashed lines. NTG, Notch target genes.

for PCP. There does appear to be an interaction between PCP and Hnf6 and/or *vhnf1*, previously known to be important in biliary development. Our data do not address where this interaction may be, other than both PCP and Hnf6 mediating biliary effects through *vhnf1*. There may be additional functional interactions between PCP and other known pathways in biliary development, such as Jagged/Notch, TGFβ, and cilia proteins. As stated above, there are well-established functional interactions between PCP and cilia proteins, and both of these pathways can affect TGFβ signaling (Guo and Wang, 2009), which is also involved with both Jagged/Notch (Guo and Wang, 2009) and HNF6 (Clotman et al., 2005) signaling. Thus, PCP appears to participate in a complex regulatory network governing biliary development (Fig. 8).

Supplementary materials related to this article can be found online at doi:10.1016/j.ydbio.2010.12.041.

Acknowledgments

The authors thank Steven EauClaire and Ashley Edens for expert technical assistance. We also thank Dr. Joshua Friedman and Dr Kathleen Loomes for critical review of the manuscript. This work was funded by the NIH (K08 DK68009), institutional support including a Foerderer-Murray award from CHOP, and the Fred and Suzanne Biesecker Pediatric Liver Center. Additionally, support was provided from the Center for Molecular Studies in Digestive and Liver Disease at the University of Pennsylvania, under P30 DK50306.

References

Ader, T., Norel, R., Levoci, L., Rogler, L.E., 2006. Transcriptional profiling implicates TGFbeta/BMP and Notch signaling pathways in ductular differentiation of fetal murine hepatoblasts. Mech. Dev. 123, 177–194.
Antic, D., Stubbs, J.L., Suyama, K., Kintner, C., Scott, M.P., Axelrod, J.D., 2010. Planar cell polarity enables posterior localization of nodal cilia and left–right axis determination during mouse and Xenopus embryogenesis. PLoS ONE 5, e8999.
Bacallao, R.L., McNeill, H., 2009. Cystic kidney diseases and planar cell polarity signaling. Clin. Genet. 75, 107–117.
Carreira-Barbosa, F., Concha, M.L., Takeuchi, M., Ueno, N., Wilson, S.W., Tada, M., 2003. Prickle 1 regulates cell movements during gastrulation and neuronal migration in zebrafish. Development 130, 4037–4046.
Ciani, L., Krylova, O., Smalley, M.J., Dale, T.C., Salinas, P.C., 2004. A divergent canonical WNT-signaling pathway regulates microtubule dynamics: dishevelled signals locally to stabilize microtubules. J. Cell Biol. 164, 243–253.
Cirone, P., Lin, S., Griesbach, H.L., Zhang, Y., Slusarski, D.C., Crews, C.M., 2008. A role for planar cell polarity signaling in angiogenesis. Angiogenesis 11, 347–360.
Clotman, F., Jacquemin, P., Plumb-Rudewiez, N., Pierreux, C.E., Van der Smissen, P., Dietz, H.C., Courtoy, P.J., Rousseau, G.G., Lemaigre, F.P., 2005. Control of liver cell fate decision by a gradient of TGF beta signaling modulated by Onecut transcription factors. Genes Dev. 19, 1849–1854.
Clotman, F., Lannoy, V.J., Reber, M., Cereghini, S., Cassiman, D., Jacquemin, P., Roskams, T., Rousseau, G.G., Lemaigre, F.P., 2002. The onecut transcription factor HNF6 is required for normal development of the biliary tract. Development 129, 1819–1828.
Coffinier, C., Gresh, L., Fiette, L., Tronche, F., Schutz, G., Babinet, C., Pontoglio, M., Yaniv, M., Barra, J., 2002. Bile system morphogenesis defects and liver dysfunction upon targeted deletion of HNF1beta. Development 129, 1829–1838.
Crosnier, C., Vargesson, N., Gschmeissner, S., Ariza-McNaughton, L., Morrison, A., Lewis, J., 2005. Delta-Notch signalling controls commitment to a secretory fate in the zebrafish intestine. Development 132, 1093–1104.
Cross, J.V., Deak, J.C., Rich, E.A., Qian, Y., Lewis, M., Parrott, L.A., Mochida, K., Gustafson, D., Vande Pol, S., Templeton, D.J., 1999. Quinone reductase inhibitors block SAPK/JNK and NFkappaB pathways and potentiate apoptosis. J. Biol. Chem. 274, 31150–31154.
Desmet, V.J., 1998. Ludwig symposium on biliary disorders: Part I. Pathogenesis of ductal plate abnormalities. Mayo Clin. Proc. 73, 80–89.
Farber, S.A., Pack, M., Ho, S.Y., Johnson, I.D., Wagner, D.S., Dosch, R., Mullins, M.C., Hendrickson, H.S., Hendrickson, E.K., Halpern, M.E., 2001. Genetic analysis of digestive physiology using fluorescent phospholipid reporters. Science 292, 1385–1388.
Fausto, N., Laird, A.D., Webber, E.M., 1995. Liver regeneration: 2. Role of growth factors and cytokines in hepatic regeneration. FASEB J. 9, 1527–1536.
Ferrante, M.I., Romio, L., Castro, S., Collins, J.E., Goulding, D.A., Stemple, D.L., Woolf, A.S., Wilson, S.W., 2009. Convergent extension movements and ciliary function are mediated by ofd1, a zebrafish orthologue of the human oral-facial-digital type 1 syndrome gene. Hum. Mol. Genet. 18, 289–303.
Field, H.A., Dong, P.D., Beis, D., Stainier, D.Y., 2003a. Formation of the digestive system in zebrafish: II. Pancreas morphogenesis. Dev. Biol. 261, 197–208.
Field, H.A., Ober, E.A., Roeser, T., Stainier, D.Y., 2003b. Formation of the digestive system in zebrafish: I. Liver morphogenesis. Dev. Biol. 253, 279–290.
Fischer, E., Legue, E., Doyen, A., Nato, F., Nicolas, J.F., Torres, V., Yaniv, M., Pontoglio, M., 2006. Defective planar cell polarity in polycystic kidney disease. Nat. Genet. 38, 21–23.
Gray, R.S., Abitua, P.B., Wlodarczyk, B.J., Szabo-Rogers, H.L., Blanchard, O., Lee, I., Weiss, G.S., Liu, K.J., Marcotte, E.M., Wallingford, J.B., Finnell, R.H., 2009. The planar cell polarity effector Fuz is essential for targeted membrane trafficking, ciliogenesis and mouse embryonic development. Nat. Cell Biol. 11, 1225–1232.
Guo, X., Wang, X.F., 2009. Signaling cross-talk between TGF-beta/BMP and other pathways. Cell Res. 19, 71–88.
Heydeck, W., Zeng, H., Liu, A., 2009. Planar cell polarity effector gene Fuzzy regulates cilia formation and Hedgehog signal transduction in mouse. Dev Dyn.
Hinton, D.E., Couch, J.A., 1998. Architectural pattern, tissue and cellular morphology in livers of fishes: relationship to experimentally-induced neoplastic responses. EXS 86, 141–164.
Ikenoya, M., Hidaka, H., Hosoya, T., Suzuki, M., Yamamoto, N., Sasaki, Y., 2002. Inhibition of rho-kinase-induced myristoylated alanine-rich C kinase substrate (MARCKS) phosphorylation in human neuronal cells by H-1152, a novel and specific Rho-kinase inhibitor. J. Neurochem. 81, 9–16.
Jing, L., Lefebvre, J.L., Gordon, L.R., Granato, M., 2009. Wnt signals organize synaptic prepattern and axon guidance through the zebrafish unplugged/MuSK receptor. Neuron 61, 721–733.
Karner, C., Wharton Jr., K.A., Carroll, T.J., 2006. Planar cell polarity and vertebrate organogenesis. Semin. Cell Dev. Biol. 17, 194–203.
Kim, S.K., Shindo, A., Park, T.J., Oh, E.C., Ghosh, S., Gray, R.S., Lewis, R.A., Johnson, C.A., Attie-Bittach, T., Katsanis, N., Wallingford, J.B., 2010. Planar cell polarity acts through septins to control collective cell movement and ciliogenesis. Science 329, 1337–1340.
Kodama, Y., Hijikata, M., Kageyama, R., Shimotohno, K., Chiba, T., 2004. The role of notch signaling in the development of intrahepatic bile ducts. Gastroenterology 127, 1775–1786.
Le Roy, C., Wrana, J.L., 2005. Clathrin- and non-clathrin-mediated endocytic regulation of cell signalling. Nat. Rev. Mol. Cell Biol. 6, 112–126.
Lokmane, L., Haumaitre, C., Garcia-Villalba, P., Anselme, I., Schneider-Maunoury, S., Cereghini, S., 2008. Crucial role of vHNF1 in vertebrate hepatic specification. Development 135, 2777–2786.
Lorent, K., Moore, J.C., Siekmann, A.F., Lawson, N., Pack, M., 2010. Reiterative use of the notch signal during zebrafish intrahepatic biliary development. Dev. Dyn. 239, 855–864.
Lorent, K., Yeo, S.Y., Oda, T., Chandrasekharappa, S., Chitnis, A., Matthews, R.P., Pack, M., 2004. Inhibition of Jagged-mediated Notch signaling disrupts zebrafish biliary development and generates multi-organ defects compatible with an Alagille syndrome phenocopy. Development 131, 5753–5766.
Lozier, J., McCright, B., Gridley, T., 2008. Notch signaling regulates bile duct morphogenesis in mice. PLoS ONE 3, e1851.
Maclean, K., Dunwoodie, S.L., 2004. Breaking symmetry: a clinical overview of left–right patterning. Clin. Genet. 65, 441–457.
Maisonneuve, C., Guilleret, I., Vick, P., Weber, T., Andre, P., Beyer, T., Blum, M., Constam, D.B., 2009. Bicaudal C, a novel regulator of Dvl signaling abutting RNA-processing bodies, controls cilia orientation and leftward flow. Development 136, 3019–3030.
Matsui, T., Raya, A., Kawakami, Y., Callol-Massot, C., Capdevila, J., Rodriguez-Esteban, C., Izpisua Belmonte, J.C., 2005. Noncanonical Wnt signaling regulates midline convergence of organ primordia during zebrafish development. Genes Dev. 19, 164–175.
Matthews, R.P., Lorent, K., Manoral-Mobias, R., Huang, Y., Gong, W., Murray, I.V., Blair, I. A., Pack, M., 2009. TNF{alpha}-dependent hepatic steatosis and liver degeneration caused by mutation of zebrafish s-adenosylhomocysteine hydrolase. Development 136, 865–875.
Matthews, R.P., Lorent, K., Pack, M., 2008. Transcription factor onecut3 regulates intrahepatic biliary development in zebrafish. Dev. Dyn. 237, 124–131.

Matthews, R.P., Lorent, K., Russo, P., Pack, M., 2004. The zebrafish onecut gene hnf-6 functions in an evolutionarily conserved genetic pathway that regulates vertebrate biliary development. Dev. Biol. 274, 245–259.
Matthews, R.P., Plumb-Rudewiez, N., Lorent, K., Gissen, P., Johnson, C.A., Lemaigre, F., Pack, M., 2005. Zebrafish vps33b, an ortholog of the gene responsible for human arthrogryposis-renal dysfunction-cholestasis syndrome, regulates biliary development downstream of the onecut transcription factor hnf6. Development 132, 5295–5306.
Mitchell, B., Stubbs, J.L., Huisman, F., Taborek, P., Yu, C., Kintner, C., 2009. The PCP pathway instructs the planar orientation of ciliated cells in the Xenopus larval skin. Curr. Biol. 19, 924–929.
Okuda, H., Miyata, S., Mori, Y., Tohyama, M., 2007. Mouse Prickle1 and Prickle2 are expressed in postmitotic neurons and promote neurite outgrowth. FEBS Lett. 581, 4754–4760.
Park, M., Moon, R.T., 2002. The planar cell-polarity gene stbm regulates cell behaviour and cell fate in vertebrate embryos. Nat. Cell Biol. 4, 20–25.
Rohrschneider, M.R., Elsen, G.E., Prince, V.E., 2007. Zebrafish Hoxb1a regulates multiple downstream genes including prickle1b. Dev. Biol. 309, 358–372.
Roskams, T., Desmet, V., 2008. Embryology of extra- and intrahepatic bile ducts, the ductal plate. Anat. Rec. (Hoboken). 291, 628–635.
Ross, A.J., May-Simera, H., Eichers, E.R., Kai, M., Hill, J., Jagger, D.J., Leitch, C.C., Chapple, J. P., Munro, P.M., Fisher, S., Tan, P.L., Phillips, H.M., Leroux, M.R., Henderson, D.J., Murdoch, J.N., Copp, A.J., Eliot, M.M., Lupski, J.R., Kemp, D.T., Dollfus, H., Tada, M., Katsanis, N., Forge, A., Beales, P.L., 2005. Disruption of Bardet–Biedl syndrome ciliary proteins perturbs planar cell polarity in vertebrates. Nat. Genet. 37, 1135–1140.
Roth-Eichhorn, S., Kuhl, K., Gressner, A.M., 1998. Subcellular localization of (latent) transforming growth factor beta and the latent TGF-beta binding protein in rat hepatocytes and hepatic stellate cells. Hepatology 28, 1588–1596.
Saburi, S., Hester, I., Fischer, E., Pontoglio, M., Eremina, V., Gessler, M., Quaggin, S.E., Harrison, R., Mount, R., McNeill, H., 2008. Loss of Fat4 disrupts PCP signaling and oriented cell division and leads to cystic kidney disease. Nat. Genet. 40, 1010–1015.
Sakaguchi, T.F., Sadler, K.C., Crosnier, C., Stainier, D.Y., 2008. Endothelial signals modulate hepatocyte apicobasal polarization in zebrafish. Curr. Biol. 18, 1565–1571.
Shimojo, M., Hersh, L.B., 2003. REST/NRSF-interacting LIM domain protein, a putative nuclear translocation receptor. Mol. Cell. Biol. 23, 9025–9031.
Song, H., Hu, J., Chen, W., Elliott, G., Andre, P., Gao, B., Yang, Y., 2010. Planar cell polarity breaks bilateral symmetry by controlling ciliary positioning. Nature 466, 378–382.
Stenkamp, D.L., Frey, R.A., 2003. Extraretinal and retinal hedgehog signaling sequentially regulate retinal differentiation in zebrafish. Dev. Biol. 258, 349–363.
Strutt, D.I., Weber, U., Mlodzik, M., 1997. The role of RhoA in tissue polarity and Frizzled signalling. Nature 15, 292–295.
Sun, Z., Hopkins, N., 2001. vhnf1, the MODY5 and familial GCKD-associated gene, regulates regional specification of the zebrafish gut, pronephros, and hindbrain. Genes Dev. 15, 3217–3229.
Takeuchi, M., Nakabayashi, J., Sakaguchi, T., Yamamoto, T.S., Takahashi, H., Takeda, H., Ueno, N., 2003. The prickle-related gene in vertebrates is essential for gastrulation cell movements. Curr. Biol. 13, 674–679.
Tamura, M., Nakao, H., Yoshizaki, H., Shiratsuchi, M., Shigno, H., Yamada, H., Ozawa, T., Totsuka, J., Hidaka, H., 2005. Development of specific Rho-kinase inhibitors and their clinical application. Biochim. Biophys. Acta 1754, 245–252.
Veeman, M.T., Slusarski, D.C., Kaykas, A., Louie, S.H., Moon, R.T., 2003. Zebrafish prickle, a modulator of noncanonical Wnt/Fz signaling, regulates gastrulation movements. Curr. Biol. 13, 680–685.
Wallace, K.N., Pack, M., 2003. Unique and conserved aspects of gut development in zebrafish. Dev. Biol. 255, 12–29.
Wallingford, J.B., Rowning, B.A., Vogeli, K.M., Rothbacher, U., Fraser, S.E., Harland, R.M., 2000. Dishevelled controls cell polarity during Xenopus gastrulation. Nature 405, 81–85.
Wang, J., Hamblet, N.S., Mark, S., Dickinson, M.E., Brinkman, B.C., Segil, N., Fraser, S.E., Chen, P., Wallingford, J.B., Wynshaw-Boris, A., 2006. Dishevelled genes mediate a conserved mammalian PCP pathway to regulate convergent extension during neurulation. Development 133, 1767–1778.
Wang, J., Mark, S., Zhang, X., Qian, D., Yoo, S.J., Radde-Gallwitz, K., Zhang, Y., Lin, X., Collazo, A., Wynshaw-Boris, A., Chen, P., 2005. Regulation of polarized extension and planar cell polarity in the cochlea by the vertebrate PCP pathway. Nat. Genet. 37, 980–985.
Yamanaka, H., Moriguchi, T., Masuyama, N., Kusakabe, M., Hanafusa, H., Takada, R., Takada, S., Nishida, E., 2002. JNK functions in the non-canonical Wnt pathway to regulate convergent extension movements in vertebrates. EMBO Rep. 3, 69–75.
Zallen, J.A., 2007. Planar polarity and tissue morphogenesis. Cell 129, 1051–1063.